

Article

C–O Hydrogenolysis of C3–C4 Polyols Selectively to Terminal Diols over Pt/W/SBA-15 Catalysts

Susmita Bhowmik ^{1,2} , Nagasuresh Enjamuri ¹ , Banu Marimuthu ^{1,2}  and Srinivas Darbha ^{1,2,*} 

¹ Catalysis and Inorganic Chemistry Division, CSIR-National Chemical Laboratory, Dr. Homi Bhabha Road, Pune 411008, Maharashtra, India

² Academy of Scientific and Innovative Research (AcSIR), Ghaziabad 201002, Uttar Pradesh, India

* Correspondence: d.srinivas@ncl.res.in; Tel.: +91-20-25902018

Abstract: Pt/W/SBA-15 catalysts (with Pt-loading = 0.5–4 wt% and W-loading = 1 wt%) prepared by the sequential impregnation method were evaluated for selective C–O cleavage of erythritol and glycerol in an aqueous medium. The Pt and W particles dispersed on SBA-15 approached close proximity at higher Pt loadings and afforded synergistic enhancement in C–O hydrogenolysis activity/selectivity. 1,4-Butanediol yields of 30.9% (at 190 °C, 50 bar H₂ and 24 h) and 1,3-propanediol yields of 34.4% (at 190 °C, 50 bar H₂ and 12 h of reaction) were obtained over these catalysts. Pt nanoparticles (facilitating dissociative H₂ adsorption and spillover) and W (present as acidic oligomeric WO_x species; activating and coordinating the polyol via 1°-OH group) worked in tandem for the selective hydrogenolysis of polyols yielding terminal diols of industrial demand.

Keywords: erythritol; glycerol; hydrodeoxygenation; diol; Pt/W/SBA-15



Citation: Bhowmik, S.; Enjamuri, N.; Marimuthu, B.; Darbha, S. C–O Hydrogenolysis of C3–C4 Polyols Selectively to Terminal Diols over Pt/W/SBA-15 Catalysts. *Catalysts* **2022**, *12*, 1070. <https://doi.org/10.3390/catal12091070>

Academic Editors: Nicolas Abatzoglou and Ajay K. Dalai

Received: 25 August 2022

Accepted: 14 September 2022

Published: 19 September 2022

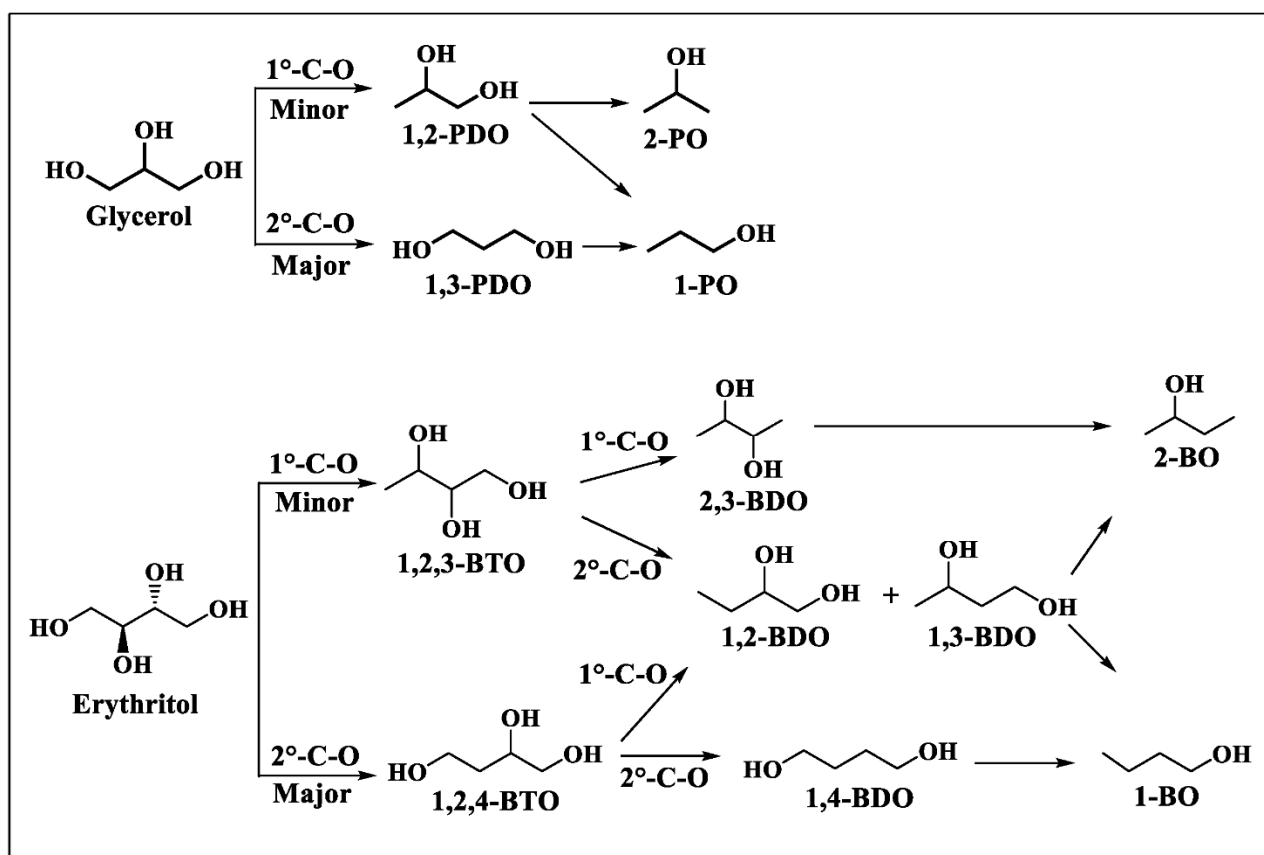
Publisher's Note: MDPI stays neutral with regard to jurisdictional claims in published maps and institutional affiliations.



Copyright: © 2022 by the authors. Licensee MDPI, Basel, Switzerland. This article is an open access article distributed under the terms and conditions of the Creative Commons Attribution (CC BY) license (<https://creativecommons.org/licenses/by/4.0/>).

1. Introduction

The rapid enhancements in global warming and depletion of fossil fuels have compelled scientists around the world to work towards alternative feedstock sources for a sustainable future. Thus, research on biomass-derived fuels and chemicals has become an area of utmost importance [1–3]. Lignocellulose (a non-edible feedstock) is the most abundant renewable biomass. Its direct conversion to fuels and fine-chemicals could achieve the goals of sustainability and net-zero carbon emissions. However, the high O/C atomic ratio of lignocellulosic biomass demands research on the development of catalysts for the efficient removal of oxygen by hydrodeoxygenation (HDO)/hydrogenolysis reactions [4,5]. Glycerol, one of the top-twelve biomass-derived platform chemicals is the by-product formed in oleochemical industries and its conversion to value-added products is a step-forward towards achieving a circular economy [6]. Hydrogenolysis of glycerol to produce propanediols (PDOs) is an important reaction as PDOs serve as important starting materials in the polymer industry (Scheme 1) [7,8]. In particular, diols with terminal hydroxyl groups are of great interest because of their vast applications. 1,3-Propanediol (1,3-PDO) is used in the production of poly(trimethylene terephthalate) (PTT). On the other hand, erythritol (meso 1,2,3,4-butanetetraol) is a C₄ sugar molecule found in fruits, fermented foods, etc., and is widely used in cosmetics, artificial sweeteners and pharmaceuticals [9]. It is mainly produced from glucose or glycerol by biochemical fermentation approaches. Conversion of erythritol to various commercially important C₄ molecules such as anhydroerythritol, butanetriols (BTOs), butanediols (BDOs) and butanols (BOs) is an eco-friendly method for the feasible production of the latter which are otherwise produced from petrochemicals [10]. 1,4-BDO is an important diol because of its extensive use in the synthesis of poly(butylene terephthalate) (PBT) polymer. 1,3-BDO is used as an organic solvent for food flavouring and as a raw material for polyurethane and polyester resins. While 1,2-BDO is used as a raw material in the production of polyester resins and plasticizers, 2,3-BDO is used in printing inks, perfumes, fumigants, etc. [11].



Scheme 1. Hydrodeoxygenation of erythritol and glycerol.

Facile production of a selective product is a major challenge in the hydrogenolysis of polyols. In glycerol hydrogenolysis, the formation of 1,3-PDO is governed by the steric hindrance and energy for the dehydration and proton affinity of hydroxyl groups [12]. Erythritol being a C4 molecule leads to the formation of a greater number of isomers and thus, yielding a selective hydrogenolysis product is highly complicated and competitive (Scheme 1). There are several reports on the development of efficient bifunctional heterogeneous catalysts for the conversion of glycerol to 1,3-PDO [7,8]. However, only a few studies are known for erythritol conversion to C4 molecules. A bifunctional, bimetallic catalyst can have synergistic interactions between the two metals which work in tandem to perform the surface-catalyzed reactions [13]. Generally, a typical hydrogenolysis bifunctional catalyst consists of a noble metal and an acidic transition metal oxide.

Rh/ReO_x/TiO₂ catalyzed the hydrogenolysis reaction of erythritol and provided BDOs with 37.5% yield at 200 °C, 25 bar H₂ and 14 h of reaction [14]. Elevated pressure (80 bar and above) was found essential for high selectivity to C4, C5 and C6 products from different polyols while using Rh/ReO_x/ZrO₂ catalysts [15]. On 3.7 wt% Rh-3.5 wt% ReO_x/ZrO₂, at an erythritol conversion of 80%, BTOs and BDOs were formed with selectivity of 37% and 29%, respectively, at 200 °C and 120 bar H₂ [16]. Rhenium-modified Ir catalysts supported on SiO₂ showed a higher selectivity to BTOs than to BDOs [17]. Ir-ReO_x catalyst supported on rutile-TiO₂ exhibited a higher selectivity to 1,4-BDO than that supported on SiO₂, especially at low conversion levels, leading to 1,4-BDO productivity of 20 mmol_{1,4-BDO}·g_{Ir}⁻¹·h⁻¹ at 100 °C and 80 bar H₂ [18]. ReO_x-Pd/CeO₂ was selective for the cleavage of vicinal -OH bonds and the formation of 1,2-BDO with a yield of 77%. 1,4-BDO was a minor diol product over this catalyst [19].

Tomishige and co-workers [20,21] studied the Pt/W catalyst supported on SiO₂ for the selective C-O cleavage of glycerol and 1,4-anhydroerythritol yielding 1,3-PDO (57 mol% at 80 h of reaction) and 1,3-BDO (54 mol% at 24 h of reaction), respectively, at

140 °C and 80 bar H₂. The interface between Pt and W (with partially reduced tungsten oxide species, +4) was invoked as an active site for the reaction. The composite catalyst, ReO_x-Au/CeO₂ + ReO_x/C, enabled the highest yield of 1,4-BDO (90%) to-date from 1,4-anhydroerythritol at 140 °C and 80 bar H₂ pressure in a non-aqueous 1,4-dioxane medium [22]. All these reports show that multi-functional catalysts with Pt/Rh/Ir (metal) and WO_x/ReO_x (metal oxide) are promising for forming terminal diols from polyols. However, high pressure (80–120 bar) and long reaction times (>24 h) are essential for good yields of 1,4-BDO. Pt/W catalysts are cheaper and more diol-yielding than Rh/ReO_x and Ir/ReO_x catalysts. According to “Metals Daily” price list (<https://www.metalsdaily.com/live-prices/pgms/>, accessed on 6 September 2022), platinum costs USD 850 per Oz while rhodium costs USD 14,000 per Oz and iridium costs USD 4750 per Oz. Cost-effective bifunctional catalysts with improved catalytic performance for the selective hydrodeoxygenation of polyols are desired.

Supports influence the physicochemical properties of metal nanoparticles and their catalytic activity. SBA-15 is an interesting silica support. Its high surface area enables controlled dispersion of metal species and its non-reducible behaviour minimizes any alteration in the electronic properties of the supported metal species due to minimal support–metal interactions. Its ordered mesoporous architecture provides facile diffusion of reactant/product molecules within the mesopores. There are a few reports on Pt/W/SBA-15 and mesoporous silica catalysts for glycerol hydrogenolysis [23–25]. To the best of our knowledge, there are no reports on the use of this catalyst for erythritol hydrogenolysis to BDOs. In this work, we screened Pt/W/SBA-15 catalysts prepared by the sequential impregnation method (first W and then Pt were loaded onto SBA-15) for glycerol and erythritol hydrogenolysis reactions. Tungsten loading was fixed at 1 wt% (as active oligomeric WO_x species are prevalent at this loading [24]) and Pt loading was varied between 0.5 and 4 wt%. The effect of the platinum weight percentage on the yield of products was studied. These catalysts were labeled as xPt/yW/SBA-15, where x refers to the wt% of Pt and y refers to the wt% of W. The catalyst, 4Pt/1W/SBA-15, was found to be superior to the others in the series enabling 1,4-BDO in yields of 30.9% and 1,3-PDO in yields of 34.5% from erythritol and glycerol, respectively, at 190 °C, 50 bar H₂ and 24 h (for erythritol) and 12 h (for glycerol) of reaction. Earlier works on SiO₂ reported that at 1 wt% loading, tungsten is in the WO_x form with moderate polymerization (oligomeric WO_x species) and with the right kind of molecular and electronic structure [20–22,24] that enables the desired acidity and electron transfer. A low W/Si ratio was reported to be advantageous. Thus, we chose such W-loading in this work and demonstrated the utility of that catalyst in the conversion of C3–C4 polyols.

2. Results and Discussion

2.1. Structure and Spectroscopic Characterization

Structural properties of the catalysts were studied by low- ($2\theta = 0.5\text{--}5^\circ$) and high-angle ($2\theta = 10\text{--}80^\circ$) X-ray diffraction (XRD) techniques. Representative XRD profiles of 2Pt/1W/SBA-15 are shown in Figure 1. These samples showed sharp, well-resolved peaks in the 2θ range of 0.6° to 2° which were indexed to reflections from (100), (110) and (200) planes of mesoporous SBA-15 with long-range, two-dimensional, hexagonal ordering and space group of *p6mm* [26]. The broad peak observed at 22.8° (in the high-angle region) was due to amorphous silica forming the pore-walls of SBA-15 and the low intensity peak at 39.7° was due to Pt nano-crystallites (JCPDS No. 65-2868). Absence of peaks at 23.6° and 33.5° suggested the absence of the crystalline monoclinic WO₃ phase in these catalysts (JCPDS card no. 043-1035). Both Pt and W species were in highly dispersed states. TEM images of the catalysts provided further evidence for the 2D hexagonal pore arrangement, long-range mesopore ordering and one-dimensional pore channel structure of SBA-15 materials (Figure 2). Pt particles had an average particle size of 7.3 ± 2.2 , 6.5 ± 2.4 , 5.6 ± 1.5 , 4.9 ± 1.4 and 3.3 ± 1.0 nm on 0.5Pt/1W/SBA-15, 1Pt/1W/SBA-15, 2Pt/1W/SBA-15, 3Pt/1W/SBA-15 and 4Pt/1W/SBA-15, respectively (Supplementary Materials, Figure S1).

The weight ratio of Pt to W influenced the size of the Pt particles. With an increase in the Pt content (from 0.5 to 4.0 wt%), the proximity between Pt and W increased and the particle size of Pt decreased. Normally, metal particle size in supported monometallic systems increases with increasing metal loading. However, the opposite trend observed in the present set of Pt/W bimetallic catalysts was due to the electronic interaction and geometric effect of W on Pt. These catalysts depicted type IV nitrogen adsorption-desorption isotherms with H1 hysteresis loop (Supplementary Materials, Figure S2) consistent with mesoporous molecular sieves. A narrow pore size distribution substantiated the uniformity of mesopores and the conclusions of TEM. 2Pt/1W/SBA-15 samples had a specific surface area of 639 m²/g, a pore volume of 1.25 cc/g and an average pore diameter of 6.4 nm. Energy dispersive X-ray spectroscopy (EDS) confirmed the presence of Pt and W in the catalyst and provided evidence for their dispersion (Supplementary Materials, Figure S3).

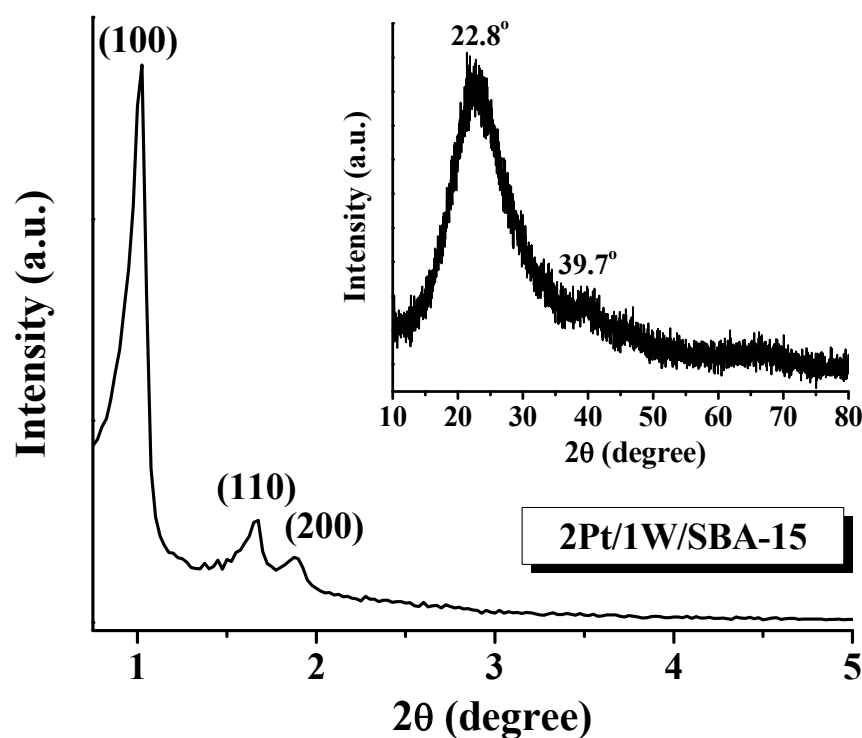


Figure 1. XRD profiles of 2Pt/1W/SBA-15 in low-angle (main panel) and high-angle (inset) regions.

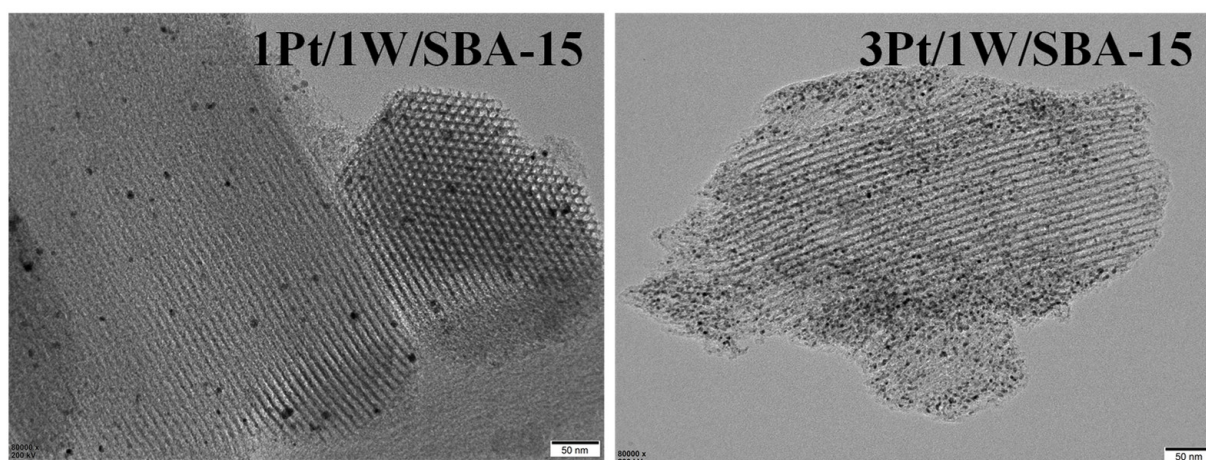


Figure 2. TEM images of 1Pt/1W/SBA-15 and 3Pt/1W/SBA-15.

These catalysts showed weak FT-Raman spectral bands at 972 and 496 cm⁻¹ due to isolated WO_x species (Supplementary Materials, Figure S4) [27,28]. The high dispersion and

low concentration (1 wt%) of tungsten are the causes for the low intensity of these tungsten features. The absence of spectral bands at 800, 705, 326, 261 and 128 cm^{-1} confirmed that tungsten in the form of WO_3 phase was not present [29]. Diffuse reflectance UV-visible spectra presented two ligand-to-metal charge transfer (LMCT; $\text{O}_{2p} \rightarrow \text{W}_{5d}$) bands at 220 and 270 nm overlapped on a broad absorption background signal. These bands at 220 and 270 nm affirmed the presence of tungsten in isolated WO_4 and oligomeric WO_x structures, respectively (Figure 3) [30]. The broad background absorption was due to metallic Pt.

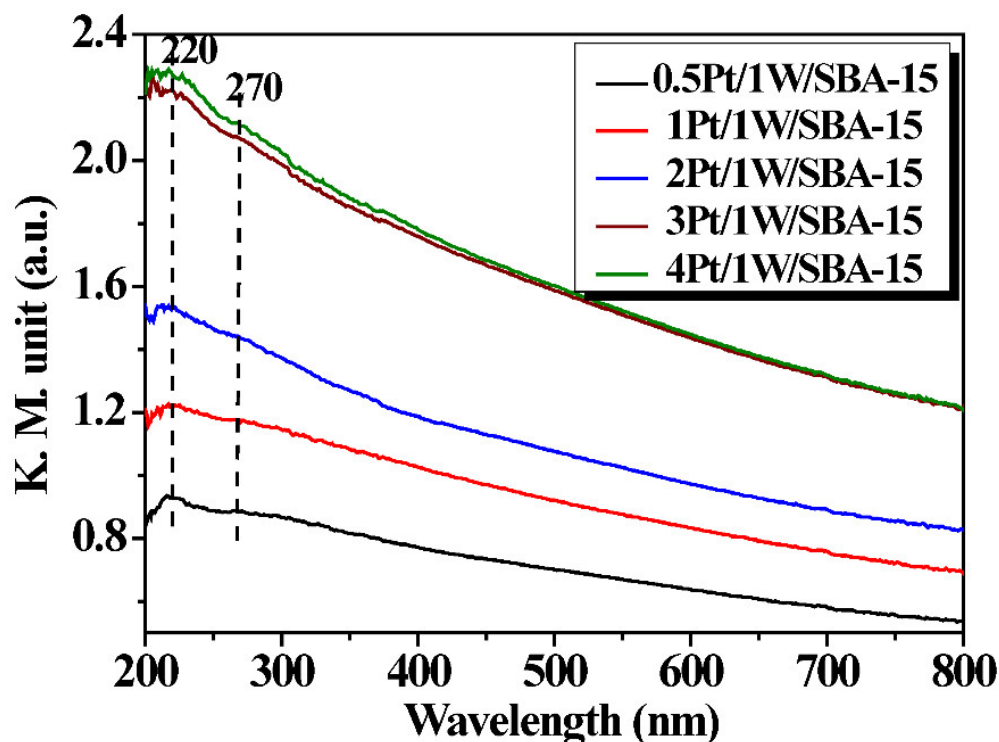


Figure 3. Diffuse reflectance UV-visible spectra of Pt/W/SBA-15 catalysts.

X-ray photoelectron (XP) spectroscopy provided information on the electronic structure and oxidation state of Pt and W species. Representative XP spectra of 4Pt/1W/SBA-15 from Pt 4f and W 4f core levels are presented in Figure 4. The Pt 4f lines appeared in the binding energy (B.E.) range of 68–78 eV and those of W 4f appeared at 34–40 eV. The spectral lines were deconvoluted and assigned as $4f_{7/2}$ and $4f_{5/2}$ spin-orbit doublet (Table 1). Based on the position of spectral lines it was concluded that Pt in these catalysts was present in the zero oxidation state and W was present in the +6 oxidation state. Any marginal changes in Pt and W XP line positions with increasing Pt content were due to changes in their close contact and changes in the particle size of Pt as noted from TEM studies. The increase in the B.E. value of Pt $4f_{7/2}$ line (from 71.2 to 71.6 eV) and decrease in the B.E. value of W $4f_{7/2}$ line (from 36.5 to 35.7 eV) was due to electron transfer from the Pt to the W species at higher Pt loadings that facilitated the synergistic catalytic hydrogenolysis activity. The structural and spectroscopic characterizations revealed that Pt and W species in these catalysts were dispersed and in improved contact at higher Pt loadings (3–4 wt%). Tungsten at 1 wt% loading was in an isolated WO_x species. Pt was in zero and W was in the +6 oxidation states.

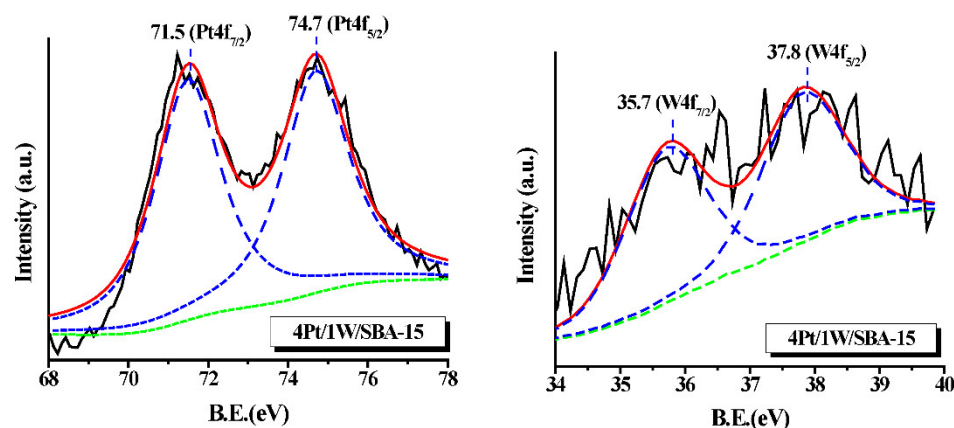


Figure 4. X-ray photoelectron spectra of 4Pt/1W/SBA-15 from Pt 4f (left) and W 4f (right) core level regions; experimental spectrum—black continuous line, simulated spectrum—red continuous line, baseline correction—green dashed line and deconvoluted spin-orbit doublet ($4f_{7/2}$ and $4f_{5/2}$) lines—blue dashed lines.

Table 1. X-ray photoelectron spectral data of Pt/W/SBA-15 catalysts.

Catalyst	B.E. (eV)			
	Pt $4f_{7/2}$	Pt $4f_{5/2}$	W $4f_{7/2}$	W $4f_{5/2}$
0.5Pt/1W/SBA-15	71.2	74.6	-	-
1Pt/1W/SBA-15	71.5	74.5	-	-
2Pt/1W/SBA-15	71.6	74.6	36.5	38.2
3Pt/1W/SBA-15	71.4	74.6	35.8	37.8
4Pt/1W/SBA-15	71.5	74.7	35.7	37.8

2.2. Catalytic Activity

2.2.1. Control Experiments and Mechanistic Pathway

The possible products in erythritol and glycerol hydrodeoxygenation (HDO) reactions are presented in Scheme 1. Cleavage of primary (1° -) and secondary (2° -) C–O bonds of erythritol yielded 1,2,3- and 1,2,4-butanetriols (1,2,3- and 1,2,4-BTOs), respectively, which on further hydrogenolysis (at 1° - and 2° -C–O positions) yielded 2,3-, 1,2-, 1,3- and 1,4-butanediols (2,3-, 1,2-, 1,3-, and 1,4-BDOs). Over-hydrogenolysis led to 2- and 1-butanols (2- and 1-BOs). Similarly, glycerol on HDO at 1° - and 2° -C–O bond positions yielded 1,2- and 1,3-propanediols (1,2- and 1,3-PDOs), respectively, which on over-hydrogenolysis yielded 2- and 1-propanols (2- and 1-POs). All these C–O cleavage products were found in the liquid-phase hydrogenolysis of erythritol and glycerol.

Control experiments were conducted to evaluate the influence of individual metal species (Pt and W) on the HDO reaction. Reduced 1W/SBA-15 (without Pt) showed poor performance with erythritol conversion of 6.2 mol% at 190 °C, 50 bar H_2 and 12 h of reaction. 1,4-Anhydroerythritol and furans (others) were the products formed (Table 2). 4Pt/SBA-15 (without W) was also not highly active. It showed erythritol conversion of 4.8 mol%. BTOs, BDOs and others were the major products and the yield of 1,4-BDO on this catalyst was 1.8 mol% only. With the bifunctional 4Pt/1W/SBA-15 catalyst, a significant enhancement in erythritol conversion to 58.1 mol% and 1,4-BDO yield to 20.1 mol% was obtained under the same reaction conditions. On extending the reaction time to 24 h, this catalyst exhibited erythritol conversion of 82.2% and 1,4-BDO yields of 30.9%. Overall BTO and BDO products selectivity was 24.1 and 50.5%, respectively (Table 2). Liu et al. [17] reported about a 32% yield (and 40% selectivity) of 1,4-BDO on 4Pt- WO_x /SiO₂ catalyst at 140 °C, 80 bar H_2 and 24 h of reaction and a 51.4% yield after 50 h of reaction. Inference derived from these control experiments suggests that the co-presence of both Pt and W species is important in the design of an active hydrogenolysis catalyst.

Table 2. Catalytic activity data 4Pt/1W/SBA-15 catalyst in the hydrodeoxygenation of erythritol ^a.

Entry	Catalyst	Erythritol Conversion (%)	Product Selectivity (%)							Yield of 1,4-BDO (%)
			BTOs		BDOs		BOs		Others	
			1,2,3-	1,2,4-	1,4-	2,3-	1-BO	2-BO		
1	1W/SBA-15	6.2	0	0	0	0	0	0	100	0
2	4Pt/SBA-15	4.8	11.6	18.4	37.1	0	0	0.4	32.5	1.8
3	4Pt/1W/SBA-15	58.1	7.4	32.2	34.8	10.1	7.4	2.8	5.3	20.2
4	4Pt/1W/SBA-15	82.2	5.8	18.3	37.6	12.9	9.2	3.3	12.9	30.9

^a Reaction conditions: Erythritol = 0.375 g, water = 12.125 g, catalyst = 0.3125 g, reaction temperature = 190 °C, H₂ pressure = 50 bar, reaction time = 12 h (for entry nos. 1–3) and 24 h (for entry no. 4), reactor volume = 50 mL, stirring speed = 600 rpm. Others include 1,4-anhydroerythritol and furans.

The synergistic interaction between Pt and W species was studied by varying the Pt-loading while the W-loading was fixed at 1 wt%. xPt/1W/SBA-15 catalysts with Pt weight percentage (x) varying from 0.5 to 4 were prepared and screened for both erythritol and glycerol hydrogenolysis. Temperature-programmed desorption of ammonia (NH₃-TPD) measurements of the catalysts (discussed later) pointed out that with increasing Pt-loading, the acidity of the catalysts increased. A significant enhancement in the conversion of both the substrates was observed (Figure 5). Glycerol conversion increased from 8.9 mol% (for 0.5Pt/1W/SBA-15) to 86.2 mol% (for 4Pt/1W/SBA-15 catalyst) (Figure 5b) and erythritol conversion increased from 3.6 mol% (for 0.5Pt/1W/SBA-15) to 58.1 mol% (for 4Pt/1W/SBA-15 catalyst) (Figure 5a). For the same set of catalysts, it was seen that the glycerol conversion percentage was much higher than erythritol conversion percentage. This can be attributed to the difference in the molecular sizes of erythritol and glycerol. BTOs and BDOs were the major products and BOs and others were the minor products in erythritol hydrogenolysis at high Pt-loadings (Figure 5a); Supplementary Materials—Table S1). The yield of 1,3-PDO increased from 2.7 mol% to 34.4 mol% (Supplementary Materials—Table S2) and that of 1,4-BDO increased from 0 to 20.2 mol% with Pt-loading increasing from 0.5 wt% to 4 wt%. These studies thus reveal that there exists a connection between the Pt-loading percentage and selectivity towards the terminal diol. At higher loading, more and more Pt was in close contact with the tungsten species and enhanced the yield of 1,4-BDO (from erythritol) and 1,3-PDO (from glycerol). Moreover, the increased acidity of the catalyst increased the rate of hydrogenolysis and dictated the course of the reaction and the selectivity of the products.

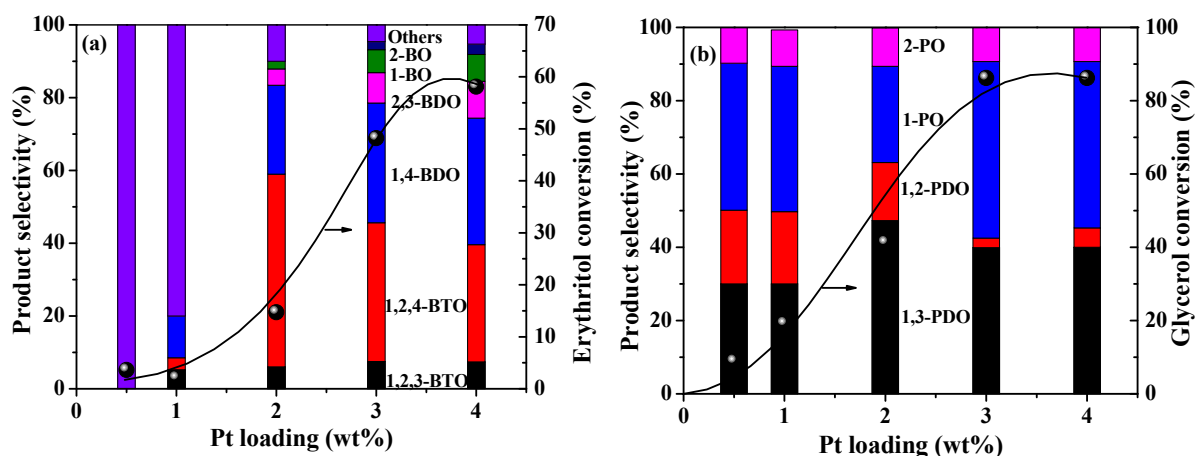
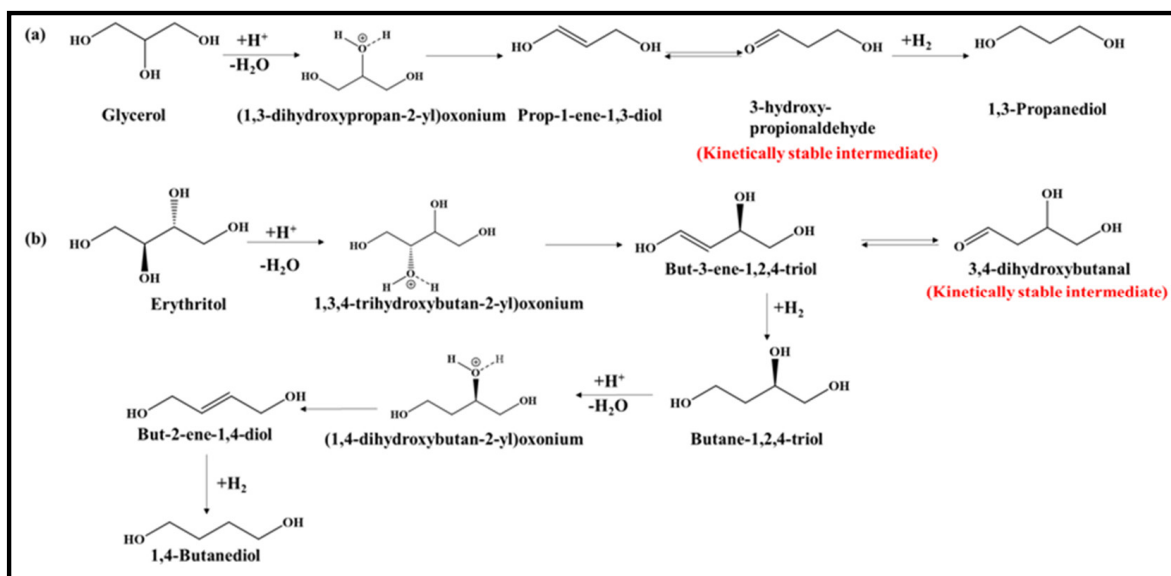


Figure 5. Influence of Pt loading on the HDO of (a) erythritol and (b) glycerol over xPt/1W/SBA-15 catalysts. Reaction conditions for (a): erythritol = 0.375 g, water = 12.125 g, catalyst = 0.3125 g, reaction temperature = 190 °C, H₂ pressure = 50 bar, reaction time = 12 h, reactor volume = 50 mL. Conditions for (b): glycerol = 0.75 g, water = 24.25 g, catalyst = 0.625 g, reaction temperature = 190 °C, H₂ pressure = 50 bar, reaction time = 12 h, reactor volume = 100 mL, stirring speed = 600 rpm.

There are several reports on Pt-WO_x/SiO₂ [17,21,24,31] wherein it has been proved that the catalysts with low tungsten loading are efficient towards production of 1,3-PDO in

high yields owing to the synergistic interaction between Pt and tungsten species and the high surface area of the SiO₂ support. The mechanistic study of products formation from glycerol has been investigated extensively. Erythritol also undergoes a hydrogenolysis reaction by dehydration followed by the hydrogenation pathway. Tomishige and co-workers [32] explained the mechanistic pathway for 1,4-BDO formation from erythritol over Ir-ReO_x/SiO₂ catalyst via a direct hydrogenolysis mechanism. However, unlike glycerol, a greater number of products are formed in erythritol hydrogenolysis and the selectivity of products solely depends on the regioselectivity of the active sites of the catalyst other than the stability of the intermediates formed. Tomishige and co-workers [17] in their study explored the possibility of obtaining diols and monoalcohols selectively from C₄–C₆ polyols while retaining the carbon chain. They concluded that the interfacial region in the Pt-WO_x system on the neutral silica support is an active site for substrate adsorption and activation. The observation can be explained by the stability of intermediates formed during the C–O hydrogenolysis reaction. Formation of 1,3-PDO occurs via the formation of 3-hydroxypropionaldehyde which is a kinetically controlled product as a secondary carbocation is generated and is much more stable. Scheme 2 shows a plausible mechanistic pathway and the stable intermediates formed in the hydrogenolysis reaction of glycerol and erythritol. The formation of 1,3-PDO and 1,4-BDO is favored because of the formation of secondary carbocation which is much more stable leading to formation of stabler products. A similar observation was inferred from the theoretical studies of Zhou et al. [33] wherein they showed that Pt/W catalysts with low amounts of tungsten were suitable. Earlier works on SiO₂ reported that Pt in contact with WO_x of moderate polymerization is more selective for C–O hydrogenolysis [20–22,24]. If Pt is supported on WO_x (as in Pt/WO_x; with WO_x having a defectiveWO₃ structure and Pt having direct contact with W), such a catalyst may show higher activity but facilitate the formation of over-hydrogenolysis products (BOs) rather than diols (BDOs) selectively.



Scheme 2. Probable mechanistic pathway for formation of major products through stable intermediates in the C–O hydrogenolysis reactions of (a) glycerol and (b) erythritol.

2.2.2. Effect of Reaction Conditions on Erythritol Hydrogenolysis

Hydrogenolysis of erythritol is a complex reaction with a potential to form multiple products. A clear picture on the course of reaction and selectivity of products can be inferred by evaluating the effect of reaction parameters. Temperature of the reaction was varied from 180 °C to 210 °C while keeping the other parameters constant (50 bar H₂ pressure and 12 h) for the entire set of experiments and it was found that temperature has a positive effect on erythritol hydrogenolysis. Conversion increased steadily from 30.8% (at 180 °C) to

73.4% (at 200 °C). Then, it dropped to 65.1% at 210 °C perhaps due to changes in the acidity of the catalyst above 200 °C (Figure 6a). The yield of 1,4-BDO followed a similar trend with its increase from 8.9% (at 180 °C) to 24.0% (at 200 °C) and post which it decreased due to over hydrogenolysis and hydrolysis forming other products. In another set of experiments, hydrogen pressure was varied from 20 to 60 bar and the reactions were conducted at 190 °C for 12 h. A positive effect of H₂ pressure was seen in the conversion values. Erythritol conversion increased from 15.9% to 58.1% and 1,4-BDO yield increased from 4.4% to 20.2% with hydrogen pressure increasing from 20 to 50 bar (Figure 6b). The increased amount of active hydrogen species available at a higher pressure of hydrogen was the cause for the higher conversion and the yield of 1,4-BDO. The further rise in pressure to 60 bar led to lowered conversion (46.8%), perhaps due to higher competition for the adsorption of erythritol and hydrogen on the active sites. Thus, 50 bar was the optimum hydrogen pressure for this reaction. Erythritol concentration in the reaction mixture was varied from 3 to 10 w% while conducting the reaction at 190 °C and 50 bar H₂ pressure for 12 h. With increasing erythritol concentration, conversion of erythritol decreased from 58.1% to 22.9% and the yield of 1,4-BDO decreased from 20.2% to 4.6% (Figure 6c). However, the amount of erythritol that was converted was about the same (0.22 g for 3 wt%, 0.201 g for 5 wt% and 0.28 g for 10 wt% concentration). Total selectivity to BTO, BDO and BOs was more than 95% at all the chosen concentrations. More and more amounts of BTOs were observed at higher erythritol concentrations due to the increased viscosity of the reaction medium. Then, with the increase in reaction time from 3 to 24 h, the conversion of erythritol increased from 21.5% to 82.2% (Figure 6d) and the yield of 1,4-BDO increased from 7.1% to 30.9%.

The variation in product selectivity confirmed that HDO of erythritol is a consecutive reaction with erythritol converting first to BTOs, which then converts to BDOs followed by BOs. High selectivity of 1,2,4-BTO, 1,4-BDO and 1-BO products provide evidence for the selective 2°-C–O bond cleavage of polyol over these catalysts.

NH₃-TPD studies showed a broad desorption peak in the temperature range of 50 to 250 °C and with a maximum peak at around 95 °C (Supplementary Materials, Figure S5). This was attributed to the presence of Lewis acid sites on the catalyst surface. On varying the catalyst from 0.5Pt/1W/SBA-15 to 4Pt/1W/SBA-15, the amount of acid sites increased from 1.99 to 4.83 μmol/g. catalyst. The amount of acidity should be the same for all the catalysts if tungsten was the only contributor to the overall acidity. However, the increase in its amount with the Pt-loading amount on the catalyst points out that both tungsten and platinum contribute to the overall acidity. A linear correlation between acidity and polyol conversion was observed which confirmed the importance of acidity in the HDO reaction. While the acid sites on W-species facilitate the adsorption of polyol through its 1°-OH group, platinum nanoparticles catalyze the dissociative adsorption of hydrogen and hydrogenolysis of 2°-C–O bond of polyol [24]. Simultaneous presence and synergistic interactions between the two active sites (Pt and W) facilitate the tandem reaction leading to terminal diols. A schematic illustration of the mechanism that brings about the synergy between the Pt and W species in 2°-C–O hydrogenolysis of erythritol over Pt/W/SBA-15 catalysts is shown in Figure 7.

A compilation of the HDO activity of different bifunctional catalysts for 1,4-BDO is presented in Table 3. A higher yield of 1,4-BDO was obtained in a non-aqueous solvent and with 1,4-anyhydroerythritol substrate. With erythritol as the substrate and water medium, Pt/W catalysts rendered a higher yield of 1,4-BDO than Pd/Re and Ir/Re catalysts. Pt/W supported on SiO₂ and SBA-15 exhibited a similar catalytic performance towards 1,4-BDO formation. Although the as-developed 4Pt/1W/SBA-15 catalysts are efficient for the hydrogenolysis of C3–C4 polyols to diols, they are not stable enough in catalyst recycling experiments due to the sintering of metal species on SBA-15 supports as a consequence of weak metal–support interactions. This necessitates further research on this topic to develop highly selective and reusable catalysts.

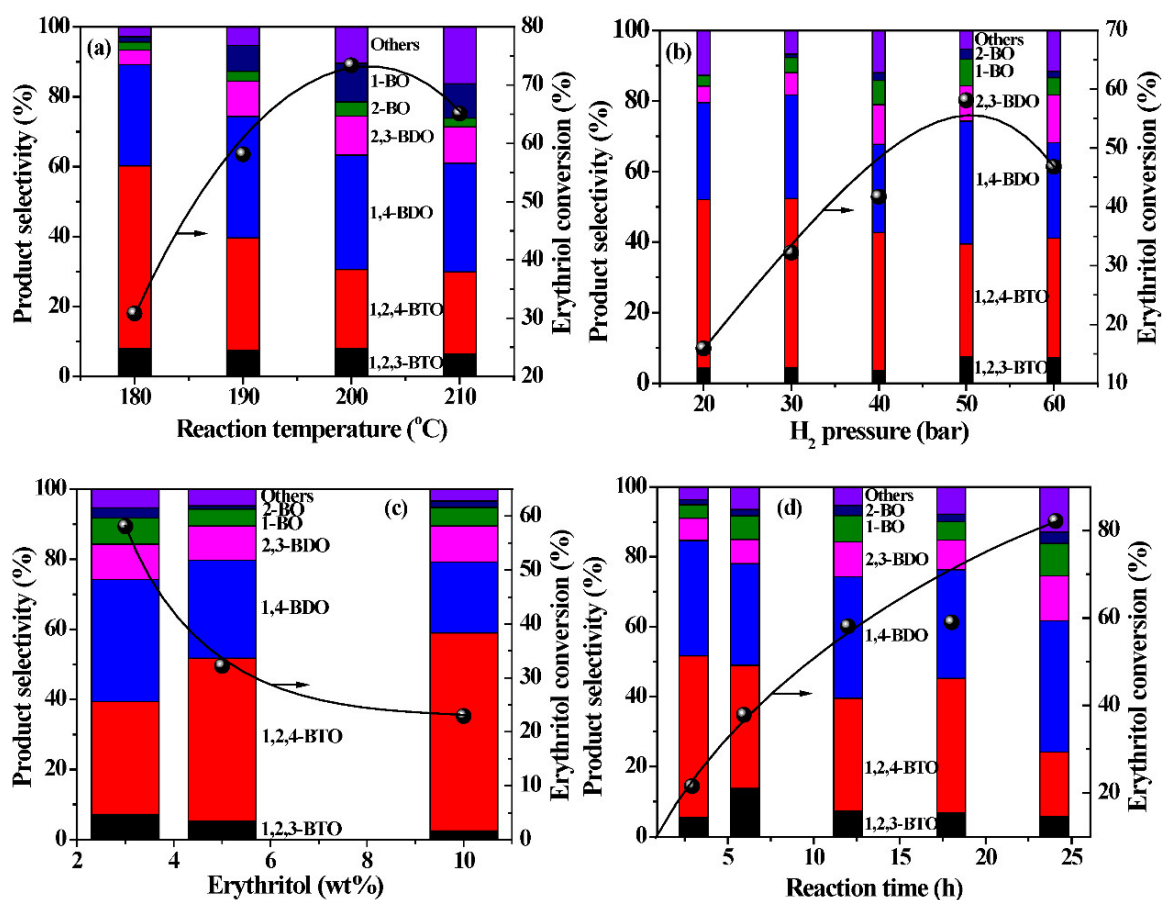


Figure 6. Influence reaction parameters: (a) reaction temperature, (b) hydrogen pressure, (c) erythritol concentration and (d) reaction time on the HDO reaction of erythritol.

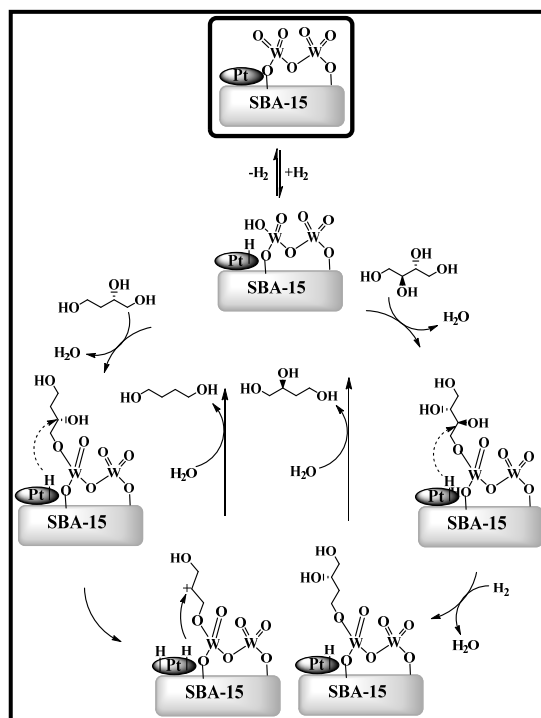


Figure 7. Proposed reaction mechanism for the hydrogenolysis of erythritol to 1,4-BDO over Pt/W/SBA-15 catalysts.

Table 3. Comparative catalytic activity data bifunctional catalyst for 1,4-BDO.

Entry	Substrate	Catalyst	Solvent	Reaction Conditions	Conversion (%)	Yield of 1,4-BDO (%)	Reference
1	Erythritol	Pt-W/SBA-15 (4 wt% Pt, 1 wt% W)	Water	Substrate = 0.375 g, H ₂ O = 12.125 g, catalyst = 0.3125 g, <i>p</i> (H ₂) = 50 bar, T = 190 °C, <i>t</i> = 24 h	82.2	30.9	Present work
2	Erythritol	Pt-WO _x /SiO ₂ (4 wt% Pt, W/Pt = 0.25)	Water	Substrate = 0.5 g, H ₂ O = 4 g, catalyst = 0.2 g, <i>p</i> (H ₂) = 80 bar, T = 140 °C, <i>t</i> = 24 h (50 h)	82 (99.3)	32 (51.4)	[17]
3	Erythritol	ReO _x -Pd/CeO ₂ (2 wt% Re, 0.3 wt% Pd)	1,4-Dioxane	Substrate = 0.5 g, 1,4-dioxane = 4g, catalyst = 0.15 g, <i>p</i> (H ₂) = 80 bar, T = 160 °C, <i>t</i> = 24 h	98	12	[19]
4	Erythritol	Ir-ReO _x /SiO ₂ (4 wt% Ir, 3.9 wt% Re)	H ₂ SO ₄ + Water	Substrate = 1 g, water = 4 g, H ₂ SO ₄ (H ⁺ /Ir = 1), catalyst = 0.3 g, <i>p</i> (H ₂) = 80 bar, T = 100 °C, <i>t</i> = 24 h	74	24	[32]
5	Erythritol	Ir-ReO _x /TiO ₂ (4 wt% Ir, 1.0 wt% Re)	Water	Substrate = 1 g, water = 4 g, catalyst = 0.3 g, <i>p</i> (H ₂) = 80 bar, T = 100 °C, <i>t</i> = 12 h	62	23	[18]
6	1,4-Anhydroerythritol	Pt-WO _x /SiO ₂ (4 wt% Pt, 0.9 wt% W)	Water	Substrate = 0.5 g, water = 4 g, catalyst = 0.2 g, <i>p</i> (H ₂) = 80 bar, T = 140 °C, <i>t</i> = 80 h	100	54	[21]
7	1,4-Anhydroerythritol	ReO _x -Au/CeO ₂ + ReO _x /C (1 wt% Re, 0.3 wt% Au; 3 wt% Re)	1,4-Dioxane	Substrate = 0.5 g, 1,4-dioxane = 4 g, catalyst = 0.15 g, <i>p</i> (H ₂) = 80 bar, T = 140 °C, <i>t</i> = 24 h	100	86	[22]
8	1,4-Anhydroerythritol	ReO _x /CeO ₂ + ReO _x /C (1 wt% Re + 3 wt% Re)	1,4-Dioxane	Substrate = 0.5 g, 1,4-dioxane = 4 g, catalyst = 0.15 g + 0.15 g, <i>p</i> (H ₂) = 80 bar, T = 140 °C, <i>t</i> = 24 h	97	83	[34]
9	1,4-Anhydroerythritol	ReO _x -Au/CeO ₂ + ReO _x /WO ₃ -ZrO ₂ (Re = 1 wt%, Au = 0.3 wt%, Re = 1 wt%, WO ₃ = 10 wt%)	1,4-Dioxane	Substrate = 0.3 g, 1,4-dioxane = 4 g, catalyst = 0.15 g + 0.15 g, <i>p</i> (H ₂) = 80 bar, T = 140 °C, <i>t</i> = 48 h	100	53	[35]

3. Materials and Methods

3.1. Catalyst Preparation

SBA-15 was prepared [26] using tetraethyl orthosilicate (Sigma-Aldrich, St. Louis, MO, USA) as the silica source, poly(ethylene glycol)-block-poly(propylene glycol)-block-poly(ethylene glycol) (EO₂₀PO₇₀EO₂₀, average molecular weight = 5800, Sigma-Aldrich) as the template and HCl (Thomas Baker, Mumbai, India) as the pH controlling agent. Bifunctional xPt/1W/SBA-15 catalysts (x refers to the weight percentage of Pt and 1 refers to the weight percentage of W) were prepared by sequential impregnation method wherein, in the first step, an appropriate amount of ammonium metatungstate (W-source, Sigma-Aldrich) was dissolved in 100 mL of Millipore water at 70 °C while stirring for 1 h. The solution was cooled to 40 °C and SBA-15 (2.5 g) was added to it. The slurry was stirred for 24 h. Then, water from it was taken out using a rotary evaporator and the solid was isolated, dried (at 110 °C for 12 h) and calcined (at 450 °C for 4 h). It was labelled as 1W/SBA-15. In the second step, 1W/SBA-15 (prepared as above) was added to a required quantity of tetraammineplatinum(II) nitrate (Pt source, Sigma-Aldrich) dissolved in 100 mL

of Millipore water at 40 °C. It was stirred for 24 h. Water was removed over a rotary evaporator and the solid was dried (at 110 °C for 12 h), calcined (at 400 °C for 4 h) and reduced in hydrogen at 350 °C for 2.5 h. It was labelled as xPt/1W/SBA-15, where x = 0.5, 1, 2, 3 and 4. For comparison, 4Pt/SBA-15 (without W) was also prepared by the impregnation method taking required amount of the Pt source and “neat” SBA-15.

3.2. Characterization Techniques

XRD studies at $2\theta = 0.5\text{--}5^\circ$ were performed on a Bruker D8 Advance X-ray diffractometer (Billerica, MA, USA) with $\text{Cu-K}\alpha$ radiation source operating at 40 kV and 30 mA, and those at $2\theta = 10\text{--}80^\circ$ were performed on a Rigaku Miniflex X-ray diffractometer (Tokyo, Japan) with a dual goniometer and $\text{Cu-K}\alpha$ radiation source operating at 30 kV and 15 mA. Nitrogen-physisorption experiments were conducted at -196°C on a Micromeritics 3Flex adsorption analyzer (Norcross, GA, USA). Prior to measurements, the catalyst samples were activated by degassing at 350 °C for 3 h. Brunauer–Emmett–Teller specific surface area (S_{BET}) of the catalyst samples was determined from the data in the relative pressure (P/P_0) range of 0.05–0.3. The total pore volume, average pore diameter and pore size distribution were determined by the Barrett–Joyner–Halenda (BJH) method. Transmission electron microscopy (TEM) images were collected on a JEM-F200 multi-purpose electron microscope (JEOL Ltd., Tokyo, Japan) fitted with a 200 kV field emission gun. Fourier transform Raman (FT-Raman) spectra were recorded on a Horiba-Jobin-Yvon LabRAM HR 800 spectrometer (Palaiseau, France) equipped with a He-Ne laser (632 nm, 20 mW). Diffuse reflectance UV-visible spectra were recorded on a Shimadzu UV-2700 spectrophotometer (Kyoto, Japan). BaSO_4 was used as reference sample. XPS measurements were conducted on a Thermo Fisher Scientific Instrument, Leicestershire, UK (Model: K-Alpha⁺) equipment using $\text{Al-K}\alpha$ anode (1486.6 eV) in a transmission lens mode and multi-channel plate (MCP) detector. The XPS lines were referenced to C_{1s} appeared at 284.8 eV and the spectra were deconvoluted using XPSPEAK41 software and Shirley background. Temperature-programmed desorption of ammonia (NH_3 -TPD) measurements were performed on a Micromeritics Autochem (model 2920) equipment. The measurements involved activation of the reduced catalyst sample in He-flow (30 mL/min) at 550 °C for 2 h, followed by cooling to 50 °C and adsorbing NH_3 in He (10 vol%), removing the physically adsorbed NH_3 species by desorbing at 50 °C for 1 h and finally collecting the TPD data in the temperature range of 50–550 °C in a programmed manner by heating at a rate of 10 °C/min. Ammonia desorption peaks were quantified using a pre-generated gas calibration file.

3.3. Reaction Procedure and Product Analysis

In a typical HDO reaction, polyol (Sigma-Aldrich) and Millipore water were taken in a 50 mL or 100 mL stainless-steel batch reactor. A known quantity of the catalyst was added to it. The reactor was capped, flushed with nitrogen (to expel out any oxygen gas present in the reactor) and then pressurized with hydrogen gas to a desired value. Temperature was raised to a desired value and the reaction was conducted for a known period of time while stirring at a speed of 600 rpm. Then, the reactor was cooled down to 25 °C. Gas was slowly vented out and the reaction mixture was collected. The catalyst was separated by centrifugation/filtration and the liquid was passed through a MS^\circledast Nylon syringe filter (diameter = 33 mm and pore size = 0.22 μm) to eliminate any catalyst particle contamination in it. Then, it was analyzed by ^1H NMR spectroscopy (in glycerol conversion reaction using a Bruker AV400 spectrometer and solvent-suppression pulse sequence (*zgpr*) method as detailed by us earlier [36]) and HPLC (in erythritol conversion reaction using a Perkin-Elmer Series 200 equipment (Waltham, MA, USA) with a refractive index detector and REZEX ROA (H^+ Organic Acid) column. A total of 0.005 M H_2SO_4 was used as the mobile phase (flow rate = 0.5 mL/min). Column temperature was maintained at 60 °C throughout the HPLC analysis). Product identification and quantification were completed by using standard samples and calibration plots.

4. Conclusions

2°-C–O bond cleavage of polyols producing terminal diols is still a challenging reaction. SBA-15-supported Pt/W catalysts (Pt = 0.5–4 wt%, W = 1 wt%) were investigated in this study for the selective hydrogenolysis of glycerol and erythritol (C3–C4 polyols) in aqueous medium to 1,3-propanediol (1,3-PDO) and 1,4-butanediol (1,4-BDO), respectively. These catalysts were prepared by the sequential impregnation method and characterized. The Pt and W particles on SBA-15 were highly dispersed (XRD, TEM, FT-Raman and diffuse reflectance UV-visible) and in close proximity at higher Pt-loading (XPS). Tungsten at 1 wt% was present in the oligomeric WO_x structure (FT-Raman). Pt was in the zero and W was in the +6 oxidation states. These catalysts were selective for 2°-C–O hydrolysis of C3–C4 polyols. A catalyst with 4 wt% Pt and 1 wt% W afforded a high yield of 1,4-BDO (30.9% at 190 °C, 50 bar H₂ and 24 h of reaction) and 1,3-PDO (34.4% at 190 °C, 50 bar H₂ and 12 h of reaction). Synergy between Pt nanoparticles and W-species rendered the selective C–O hydrogenolysis activity of these catalysts. Pt/W supported on silica materials (SiO₂ and SBA-15) are promising catalysts providing high yields of terminal diols.

Supplementary Materials: The following supporting information can be downloaded at: <https://www.mdpi.com/article/10.3390/catal12091070/s1>, Figure S1: Pt particle size distribution profiles; Figure S2: N₂-physisorption isotherms; Figure S3: High-angle annular dark field image and elemental mapping; Figure S4: FT-Raman spectrum of 2Pt/1W/SBA-15; Figure S5: NH₃-TPD profiles; Table S1: Catalytic activity data for erythritol hydrogenolysis; Table S2: Catalytic activity data of glycerol hydrogenolysis.

Author Contributions: Conceptualization, S.D.; methodology, S.D., S.B. and N.E.; formal analysis, S.B. and N.E.; investigation, S.B. and N.E.; data curation, S.B. and N.E.; writing—original draft preparation, S.B. and N.E.; writing—review and editing, S.D.; supervision, S.D. and B.M.; project administration, S.D. and B.M.; funding acquisition, S.D. All authors have read and agreed to the published version of the manuscript.

Funding: This research was funded by Council of Scientific and Industrial Research, India under CSIR-Bhatnagar Fellowship grant number SSB000926; P90807.

Data Availability Statement: Not applicable.

Acknowledgments: S.D. acknowledges the Council of Scientific and Industrial Research (CSIR), New Delhi for the award of CSIR-Bhatnagar Fellowship (SSB 000926; P90807). Authors thank Ankur Bordoloi, CSIR-Indian Institute of Petroleum, Dehradun for the help in NH₃-TPD measurements.

Conflicts of Interest: The authors declare no conflict of interest. The funders had no role in the design of the study; in the collection, analyses, or interpretation of data; in the writing of the manuscript; or in the decision to publish the results.

References

1. Alonso, D.M.; Bond, J.Q.; Dumesic, J.A. Catalytic Conversion of Biomass to Biofuels. *Green Chem.* **2010**, *12*, 1493–1513. [[CrossRef](#)]
2. Ruppert, A.M.; Weinberg, K.; Palkovits, R. Hydrogenolysis Goes Bio: From Carbohydrates and Sugar Alcohols to Platform Chemicals. *Angew. Chem. Int. Ed.* **2012**, *51*, 2564–2601. [[CrossRef](#)] [[PubMed](#)]
3. Besson, M.; Gallezot, P.; Pinel, C. Conversion of Biomass into Chemicals over Metal Catalysts. *Chem. Rev.* **2014**, *114*, 1827–1870. [[CrossRef](#)] [[PubMed](#)]
4. Yun, Y.S.; Berdugo-Díaz, C.E.; Flaherty, D.W. Advances in Understanding the Selective Hydrogenolysis of Biomass Derivatives. *ACS Catal.* **2021**, *11*, 11193–11232. [[CrossRef](#)]
5. Tomishige, K.; Yabushita, M.; Cao, J.; Nakagawa, Y. Hydrodeoxygenation of Potential Platform Chemicals Derived from Biomass to Fuels and Chemicals. *Green Chem.* **2022**, *24*, 5652–5690. [[CrossRef](#)]
6. Top Value Added Chemicals from Biomass, Vol. 1—Results of Screening for Possible Candidates from Sugars and Synthesis Gas, U.S. Department of Energy: Energy Efficiency and Renewable Energy. Available online: <https://www.nrel.gov/docs/fy04osti/35523.pdf> (accessed on 1 August 2022).
7. Bhowmik, S.; Darbha, S. Advances in Solid Catalysts for Selective Hydrogenolysis of Glycerol to 1,3-Propanediol. *Catal. Rev. Sci. Eng.* **2021**, *63*, 639–703. [[CrossRef](#)]

8. Dias da Silva Ruy, A.; Maria de Brito Alves, R.; Lewis Reis Hower, T.; De Aguiar Pontes, D.; Sena Gomes Teixeira, L.; Antônio Magalhães Pontes, L. Catalysts for Glycerol Hydrogenolysis to 1,3-Propanediol: A Review of Chemical Routes and Market. *Catal. Today* **2021**, *381*, 243–253. [[CrossRef](#)]
9. Nakagawa, Y.; Kasumi, T.; Ogihara, J.; Tamura, M.; Arai, T.; Tomishige, K. Erythritol: Another C4 Platform Chemical in Biomass Refinery. *ACS Omega* **2020**, *5*, 2520–2530. [[CrossRef](#)]
10. Weitz, H.M.; Schnabel, R.; Platz, R. Preparation of Butane-1,4-diol. U.S. Patent No. 4361710, 30 November 1982.
11. Ji, X.J.; Huang, H.; Ouyang, P.K. Microbiol 2,3-Butanediol Production: A State-of-the-Art Review. *Biotechnol. Adv.* **2011**, *29*, 351–364. [[CrossRef](#)]
12. Nimlos, M.R.; Blanksby, S.J.; Qian, X.; Himmel, M.E.; Johnson, D.K. Mechanisms of Glycerol Dehydration. *J. Phys. Chem. A* **2006**, *110*, 6145–6156. [[CrossRef](#)]
13. Robinson, A.M.; Hensley, J.E.; Medlin, J.W. Bifunctional Catalysts for Upgrading of Biomass-Derived Oxygenates: A Review. *ACS Catal.* **2016**, *6*, 5026–5043. [[CrossRef](#)]
14. Virgilio, E.M.; Padró, C.L.; Sad, M.E. Butanediols Production from Erythritol on Rh Promoted Catalyst. *Lat. Am. Appl. Res.* **2020**, *50*, 89–94.
15. Sadier, A.; Perret, N.; Da Silva Perez, D.; Besson, M.; Pinel, C. Effect of Carbon Chain Length on Catalytic C–O Bond Cleavage of Polyols over Rh-ReO_x/ZrO₂ in Aqueous Phase. *Appl. Catal. A Gen.* **2019**, *586*, 117213. [[CrossRef](#)]
16. Said, A.; Da Silva Perez, D.; Perret, N.; Pinel, C.; Besson, M. Selective C–O Hydrogenolysis of Erythritol over Supported Rh-ReO_x Catalysts in the Aqueous Phase. *ChemCatChem* **2017**, *9*, 2768–2783. [[CrossRef](#)]
17. Liu, L.; Cao, J.; Nakagawa, Y.; Betchaku, M.; Tamura, M.; Yabushita, M.; Tomishige, K. Hydrodeoxygenation of C4–C6 Sugar Alcohols to Diols or Mono-Alcohols with Retention of the Carbon Chain Over a Silica-Supported Tungsten Oxide-Modified Platinum Catalyst. *Green Chem.* **2021**, *23*, 5665–5679. [[CrossRef](#)]
18. Gu, M.; Lice, L.; Nagakawa, Y.; Li, C.; Tamura, M.; Shen, Z.; Zhou, X.; Zhang, Y.; Tomishige, K. Selective Hydrogenolysis of Erythritol Over Ir-ReO_x/Rutile-TiO₂ Catalyst. *ChemSusChem* **2021**, *14*, 642–654. [[CrossRef](#)]
19. Ota, N.; Tamura, M.; Nakagawa, Y.; Okumura, K.; Tomishige, K. Hydrodeoxygenation of Vicinal OH Groups over Heterogeneous Rhenium Catalyst Promoted by Palladium and Ceria Support. *Angew. Chem. Int. Ed.* **2015**, *54*, 1897–1900. [[CrossRef](#)]
20. Liu, L.; Asano, T.; Nakagawa, Y.; Gu, M.; Li, C.; Tamura, M.; Tomishige, K. Structure and Performance Relationship of Silica-Supported Platinum-Tungsten Catalysts in Selective C–O Hydrogenolysis of Glycerol and 1,4-Anhydroerythritol. *Appl. Catal. B Environ.* **2021**, *292*, 120164. [[CrossRef](#)]
21. Liu, L.; Asano, T.; Nakagawa, Y.; Tamura, M.; Tomishige, K. One-Pot Synthesis of 1,3-Butanediol by 1,4-Anhydroerythritol Hydrogenolysis Over a Tungsten-Modified Platinum on Silica Catalysts. *Green Chem.* **2020**, *22*, 2375–2380. [[CrossRef](#)]
22. Wang, T.; Liu, S.; Tamura, M.; Nakagawa, Y.; Hiyoshi, N.; Tomishige, K. One-Pot Catalytic Selective Synthesis of 1,4-Butanediol from 1,4-Anhydroerythritol and Hydrogen. *Green Chem.* **2018**, *20*, 2547–2557. [[CrossRef](#)]
23. ShanthiPriya, S.; PavanKumar, V.; Lakshmi Kantam, M.; Bhargava, S.K.; Srikanth, A.; Chary, K.V.R. High Efficiency Conversion of Glycerol to 1,3-Propanediol Using a Novel Platinum–Tungsten Catalyst Supported on SBA-15. *Ind. Eng. Chem. Res.* **2015**, *54*, 9104–9115.
24. Fan, Y.; Cheng, S.; Wang, H.; Ye, D.; Xie, S.; Pei, Y.; Hu, H.; Hua, W.; Li, Z.H.; Qiao, M.; et al. Nanoparticulate Pt on Mesoporous SBA-15 Doped with Extremely Low Amount of W as a Highly Selective Catalyst for Glycerol Hydrogenolysis to 1,3-Propanediol. *Green Chem.* **2017**, *19*, 2174–2183. [[CrossRef](#)]
25. Feng, S.; Zhao, B.; Liang, Y.; Liu, L.; Dong, J. Improving Selectivity to 1,3-Propanediol for Glycerol Hydrogenolysis Using W- and Al-Incorporated SBA-15 as Support for Pt Nanoparticles. *Ind. Eng. Chem. Res.* **2019**, *58*, 2661–2671. [[CrossRef](#)]
26. Zhao, D.; Feng, J.; Huo, Q.; Melosh, N.; Fredrickson, G.H.; Chmelka, B.F.; Stucky, G.D. Triblock Copolymer Syntheses of Mesoporous Silica with Periodic 50 to 300 Å Pores. *Science* **1998**, *279*, 548–552. [[CrossRef](#)] [[PubMed](#)]
27. Ross-Medgaarden, E.I.; Wachs, I.E. Structural Determination of Bulk and Surface Tungsten Oxides with UV–Vis Diffuse Reflectance Spectroscopy and Raman Spectroscopy. *J. Phys. Chem. C* **2007**, *111*, 15089–15099. [[CrossRef](#)]
28. Horsley, J.A.; Wachs, I.E.; Brown, J.M.; Via, G.H.; Hardcastle, F.D. Structure of Surface Tungsten Oxide Species in the Tungsten Trioxide/Alumina Supported Oxide System from X-Ray Absorption Near-Edge Spectroscopy and Raman Spectroscopy. *J. Phys. Chem.* **1987**, *91*, 4014–4020. [[CrossRef](#)]
29. Barton, D.G.; Shtein, M.; Wilson, R.D.; Soled, S.L.; Iglesia, E. Structure and Electronic Properties of Solid Acids Based on Tungsten Oxide Nanostructures. *J. Phys. Chem. B* **1999**, *103*, 630–640. [[CrossRef](#)]
30. Guntida, A.; Suriye, K.; Panpranot, J.; Praserttham, P. Lewis Acid Transformation to Brønsted Acid Sites over Supported Tungsten Oxide Catalysts Containing Different Surface WO_x Structures. *Catal. Today* **2020**, *358*, 354–369. [[CrossRef](#)]
31. Cheng, S.; Fan, Y.; Zhang, X.; Zeng, Y.; Xie, S.; Pei, Y.; Zeng, G.; Qiao, M.; Zong, B. Tungsten-Doped Siliceous Mesocellular Foams-Supported Platinum Catalyst for Glycerol Hydrogenolysis to 1,3-Propanediol. *Appl. Catal. B Environ.* **2021**, *297*, 120428. [[CrossRef](#)]
32. Amada, Y.; Watanabe, H.; Hirai, Y.; Kajikawa, Y.; Nakagawa, Y.; Tomishige, K. Production of Biobutanediols by the Hydrogenolysis of Erythritol. *ChemSusChem* **2012**, *5*, 1991–1999. [[CrossRef](#)]
33. Zhou, W.; Li, Y.; Wang, X.; Yao, D.; Wang, Y.; Huang, S.; Li, W.; Zhao, Y.; Wang, S.; Ma, X. Insight into the Nature of Brønsted Acidity of Pt-(WO_x)_n-H Model Catalysts in Glycerol Hydrogenolysis. *J. Catal.* **2020**, *388*, 154–163. [[CrossRef](#)]

34. Wang, T.; Tamura, M.; Nakagawa, Y.; Tomishige, K. Preparation of Highly Active Monometallic Rhenium Catalysts for Selective Synthesis of 1,4-Butanediol from 1,4-Anhydroerythritol. *ChemSusChem* **2019**, *12*, 3615–3626. [[CrossRef](#)] [[PubMed](#)]
35. Wang, T.; Nakagawa, Y.; Tamura, M.; Okumura, K.; Tomishige, K. Tungsten–Zirconia-Supported Rhenium Catalyst Combined with a Deoxy Dehydration Catalyst for the One-Pot Synthesis of 1,4-Butanediol from 1,4-Anhydroerythritol. *React. Chem. Eng.* **2020**, *5*, 1237–1250. [[CrossRef](#)]
36. Bhowmik, S.; Enjamuri, N.; Darbha, S. Hydrogenolysis of Glycerol in an Aqueous Medium over Pt/WO₃/Zirconium Phosphate Catalysts Studied by ¹H NMR Spectroscopy. *New J. Chem.* **2021**, *45*, 5013–5022. [[CrossRef](#)]